Astron. Astrophys. 276, 117–128 (1993)

ASTRONOMY AND ASTROPHYSICS

The 0.1-2.5 keV X-ray spectrum of the O4f star ζ Puppis

D.J. Hillier[1], R.P. Kudritzki[1,2], A.W. Pauldrach[1], D. Baade[3], J.P. Cassinelli[4], J. Puls[1], and J.H.M.M. Schmitt[5]

[1] Institut für Astronomie und Astrophysik, Scheinerstrasse 1, W-8000 München 80, Germany
[2] Max-Planck-Institut für Astrophysik, Karl-Schwarzschild-Str. 1, W-8046 Garching bei München, Germany
[3] European Southern Observatory, Karl-Schwarzschild-Str. 2., W-8046 Garching bei München, Germany
[4] Washburn Observatory, University of Wisconsin-Madison, USA
[5] Max-Planck-Institut für Extraterrestrische Physik, W-8046 Garching bei München, Germany

Received December 11, 1992; accepted February 6, 1993

Abstract. We have obtained a high quality ROSAT PSPC spectrum of the bright O4 f star ζ Pup. Allowing for the wind X-ray opacity, as computed from detailed non-LTE stellar wind models of ζ Pup, and under the assumption that the X-rays arise from shocks distributed throughout the wind, we have been able to match the observed X-ray spectrum (0.1 to 2.5keV).

The best model fit is obtained when He^{++} recombines to He^{+} in the outer regions of the stellar wind, as predicted by recent detailed cool wind model calculations. With a single temperature plasma, the best model fit indicates a temperature of $\log T_s(K) = 6.5$ to 6.6 corresponding to shock velocities of around 500 km s^{-1}. A 2 temperature plasma yields a significantly improved fit, and indicates temperatures of $\log T_s(K) =$ 6.2 and 6.7 for the 2 components. The hotter component accounts for 55% of the intrinsic (75% of the observed) X-ray flux. Due to absorption by the stellar wind, and to a minor extent stellar occultation, less than 5% of the total emitted X-ray flux escapes the star. The models require significant X-ray emission (particularly at energies less than 0.5 keV) from large radii ($r > 100R_*$).

In models without recombination, the fits, even with a 2 temperature plasma, are unacceptable. A significant K shell absorption is predicted by these models, but is definitely not present in the observational data. The analysis suggests that the X-ray flux provides an invaluable diagnostic of the ionization of helium in the stellar wind of stars with low reddening.

Key words: stars: individual: ζ Pup, – stars: early-type – stars: mass-loss – X-rays: stars

1. Introduction

The detection of X-rays from O stars was one of the first spectacular discoveries of the *Einstein* Observatory. X-ray imaging of the Carina Nebula in the neighborhood of η Car revealed η Car, a WR star, and five O stars (Seward et al. 1979). Similarly, 4 of the most luminous O stars were detected by Harnden et al. (1979) in the heavily obscured OB association VI Cygni. The detection of X-rays from O stars was not unexpected; Cassinelli & Olson (1979) had invoked them to explain the anomalous ionization observed in O and early B stars.

A catalogue of all O stars observed (many serendipitously) by the *Einstein* satellite was compiled by Chlebowski et al. (1989, hereafter CHS). As earlier results had shown (e.g., Seward et al. 1979; Long & White 1980; Pallavicini et al. 1981), the X-ray luminosity (L_X) was found to scale as the bolometric luminosity (L_{BOL}). The ratio of L_X to L_{BOL} is typically 10^{-7} but shows a large scatter of ± 1 dex.

An extensive analysis of the O stars data set was performed by Chlebowski (1989). He claimed that 3 factors appear to influence the observed X-ray luminosity:

1. Binarity — binary systems were found to be significantly brighter (about a factor of 2) than single O stars.
2. Non-thermal radio emission — stars classified as non-thermal radio emitters were strong X-ray sources.
3. Environment — runaway O stars are typically a factor of 2 fainter than non-runaway O stars, whereas stars in dense clouds tend to be brightest.

While the first 2 factors are not surprising, the observed correlation of X-ray luminosity with environment is unexpected. HRI observations (e.g., CHS) show the sources to generally be unresolved ($\theta < 5''$), and hence the X-rays could not come from an interaction of the O star with its environment: A massive star that has a strong stellar wind will have cleared out nearby material on a fairly short time scale. This restriction led Chlebowski (1989) to propose that the X-rays were produced by the interaction of the stellar wind with dense condensations, possibly remnants from protostellar clouds.

A more recent analysis of X-ray emission from O type stars has been performed by Sciortino et al. (1990). They suggest that there is no evidence for a correlation between X-ray emission

Send offprint requests to: D. J. Hillier

and environment. However, they do find evidence for a correlation of L_X with wind momentum ($\dot{M}V_\infty$), and make the interesting suggestion that this correlation is the most fundamental; the correlation between L_X and L_{BOL} being a consequence of the relationship between luminosity and wind momentum.

There are several difficulties with the *Einstein* X-ray data which may have limited the validity of the X-ray analyses.

First, the CHS sample is not well defined, and hence may be influenced by various selection effects. In particular, a plot of L_X/L_{BOL} versus m_{BOL} using the data from the CHS catalogue shows a loose correlation (r=0.6, with 69 data points) which suggests that Malmquist bias may be influencing the results.

Second, many O stars are reddened, requiring that the observed X-ray luminosities be corrected for interstellar extinction. Only for a fraction of the sample were reliable interstellar measurements of the hydrogen column density (N_H) available. For other stars, the N_H were derived from the E_{B-V} values using the correlation of N_H with E_{B-V}.

Third, no correction for internal wind absorption was made. Unfortunately, such corrections are model dependent and hence it could be argued that the observed X-ray luminosities (corrected only for interstellar absorption) are more fundamental. However, we believe the intrinsic X-ray emission of the wind (i.e., what we would observe in the absence of occultation effects, wind absorption, and interstellar absorption) to be more fundamental as it is this quantity that any X-ray production mechanism must account for, and it this quantity which influences the ionization structure. The X-ray emission region probably has no direct relationship to the region where the X-ray absorption occurs — it is the 'smooth wind' rather than the X-ray emission regions themselves which produces most of the attenuation.

Although several models, with differing intrinsic X-ray luminosities, could give rise to the same observed flux, it is to be hoped that such models can be distinguished by the validity of their physical assumptions, and by their different influences on the optical and UV spectrum.

With the advent of the X-ray satellite ROSAT, with its superior energy resolution and sensitivity, we decided to reinvestigate the X-ray properties of O stars by observing a well defined sample of 41 objects covering most spectral and luminosity classes. Here, we wish to report on ROSAT observations of one member of this sample, the bright O star ζ Pup. This serves two purposes. First it lays the groundwork for subsequent analysis of the other sample members. Second, ζ Pup is used as the standard in 'O star' analyses. It is therefore crucial to understand the origin of X-rays in this object, and how they (and the associated extreme-UV radiation field) may influence stellar diagnostics.

2. X-ray production in O stars

No definitive model for the X-ray production in the winds of O stars is available. Several different models have been proposed for X-ray production but all involve free parameters and make untested assumptions. In order to provide a basis for our analyses in Sect. 4, and to lay the foundations for subsequent analyses and papers, we present the basic scenarios that have been proposed for X-ray production in massive stars. In doing so, we discuss previous observations, both optical (or UV) and X-ray, which constrain these scenarios.

2.1. The hot coronal model

The possible existence of a corona in massive stars (both Of and WR) was originally suggested because of the difficulty in explaining the observed emission lines seen in their spectra. A difficulty arose , however, because of the lack of a strong convection zone which is believed to be essential for the generation of the solar corona. Hearn (1972) postulated radiation driven sound waves as a possible mechanism for generating hot coronae in massive stars.

The existence of a corona in massive stars gained credence when Cassinelli & Olson (1979) invoked them to explain the anomalous ionization observed in O and B stars. Rogerson & Lamers (1975), for example, had shown that lines arising from very high ionization species existed in the spectra of the B star τ Sco. It was generally believed, but not shown with detailed modeling, that the observed ionization could not be produced by the photospheric radiation field. Cassinelli & Olson (1979) showed that X-rays arising from an inner thin coronal zone, with a temperature of 5×10^6 K, could reproduce, through Auger ionization, the ionization stages observed in the cool wind.

The thin coronal model has been further refined and elaborated on by Waldron (1984). He notes that because of the overlying wind absorption, the incident X-ray fluxes at the base of the wind could be 3 to 4 orders of magnitude larger than that which escapes.

Pauldrach (1987) questioned the need for X-rays to explain the observed ionization stages in ζ Pup. He argued that the anomalous ionization seen in ζ Pup could be explained by the standard NLTE wind model without invoking X-rays, or a high wind temperature. More recent models, however, suggest that X-rays (or at least the associated extreme UV emission) are required to match the observed P Cygni profiles (Pauldrach et al. 1993). These current wind models provide a good qualitative fit to the observed spectrum of ζ Pup.

If an inner coronal zone is present, it should manifest itself in the behavior of lines formed deep in the wind (velocities from the photosphere to 200 km s^{-1}). These lines should show profiles incompatible with the standard wind model. Such a procedure has already been used to limit the extent of the corona by Cassinelli et al. (1978), who analyzed the Hα emission profile in ζ Pup. The new generation of radiation driven wind models should be better equipped to reveal such discrepancies, and hence place tighter limits on the structure of the corona region. Any X-ray production mechanism is only viable provided that its influence on the UV and optical spectrum remains consistent with observations.

The coronal models suffer from 3 serious objections. First, they predict severe attenuation of soft X-rays which is not observed. The strongest constraints come from observations of

several O stars (unfortunately not including ζ Pup) with the solid-state spectrometer. These observations show no evidence for absorption at the 0.6 keV K shell ionization edge of Oxygen (Cassinelli & Swank 1983) — absorption which is predicted in the coronal models to be very strong.

A second argument against the coronal wind model comes from the work of Nordsieck et al. (1981) who searched for coronal [Fe XIV]530.3 nm line emission in the optical spectrum of ϵ Orionis (B0 Ia) and κ Orionis (B0.5 Ia). No coronal emission was detected, and their upper limit led them to conclude that at least some of the observed X-rays arise from sources distributed in the wind.

A more stringent limit on coronal X-ray emission was obtained by Baade & Lucy (1987), who searched for [Fe XIV]530.3nm line emission in ζ Pup. No coronal emission was detected, and their upper limit led them to conclude that a base coronal model could be eliminated, and that X-rays are most probably formed within the cool wind.

A final weakness of the coronal model is that no mechanism has been demonstrated to account for both the generation and maintenance of the hot coronal zone.

2.2. The Lucy and White shock model

Because the coronal models have difficulties in explaining the X-ray spectra of O stars, Lucy & White (1980), developed a phenomenological theory for the production of X-rays in the stellar wind. The X-rays are assumed to arise from hot gas coexisting with the "normal" cool stellar wind. The production of the hot gas was postulated to be a direct consequence of the inherent instability of radiation driven winds (see Sect. 2.3).

The Lucy and White model also has difficulties in explaining the observed X-ray absorption (Cassinelli & Swank 1983), since it also predicts significant attenuation. An improved shock model was put forward by Lucy (1982b). In this refined model, the shocks could exist well out into the terminal flow, and consequently the X-rays would suffer much less attenuation than in the coronal model, or in the original Lucy & White (1980) model.

The only free parameter in the Lucy (1982b) model is the velocity separation of the shocks, which he characterizes by a dimensionless parameter ν; plausibility arguments suggest that ν is in the range 0.4 to 1. Lucy (1982b) noted that the preferred value of ν yielded X-ray luminosities that were too small by at least an order of magnitude, and spectra that were too soft. He suggested that a distribution of shock strengths might overcome these difficulties.

A detailed comparison of the Lucy model with observations of ϵ Ori was made by Cassinelli & Swank (1983). They confirmed that a value of ν in the suggested range led to X-rays that were too soft, and too few, to account for the observations. If a fraction of the shocks (1 in 200) were strong (i.e., ν = 3.4) an acceptable fit could be obtained, however Cassinelli & Swank (1983) noted this would lead to strong variability in the high energy tail which is not observed.

2.3. The OCR shock model

As noted previously, radiation driven winds are inherently unstable. The instability was first suggested by Lucy & Solomon (1970) and has been investigated further by MacGregor et al. (1979), Carlberg (1980), Abbott (1980), and Lucy (1984). The most detailed one dimensional analyses of the line-driven instability are by Owocki & Rybicki (1984, 1985, 1986), while perturbations in three dimensions have been discussed by Rybicki et al. (1990).

In order to further investigate the consequence of the line-driven instabilities on stellar winds, Owocki et al. (1988) (hereafter OCR) performed detailed time dependent hydrodynamical calculations of radiation driven winds. Their calculations show that the instability naturally leads to the production of large amplitude shocks (up to 1000 $\mathrm{km\,s^{-1}}$). A particularly important result of their work is the structure of the shocks. Their models predict that the *reverse shock* is much stronger than the *forward shock*, just the opposite to what is assumed in the phenomenological shock model of Lucy & White (1980), and Lucy (1982b). The OCR shock structure, in which the high velocity gas has low density, appears to be more consistent with the observed shape of the P Cygni absorption in UV resonance profiles (Puls et al. 1993).

Because the OCR calculations do not include an energy equation, and further assume an isothermal wind (an assumption which breaks down at low densities (see Sect. 5)), the current generation of models cannot be used to predict the X-ray spectra of O stars. In addition, present model calculations extend to only a few R_*, whereas a prediction of the X-ray spectrum also requires a prediction of the shock structure at much larger radii (Sect. 4). A further problem is that the calculations are one dimensional — is the time averaged X-ray spectrum in a one dimensional model equivalent to the X-ray spectrum (not necessarily time averaged) of a full multi-dimensional model?

Since radiation winds are theoretically unstable, and since the instability probably manifests itself by the observed variability of the wind lines, the large turbulent velocities needed to fit the absorption components of P Cygni profiles, and the presence of narrow components, it is natural to ascribe the production of the X-rays as in some way related to this instability. Unfortunately a great deal of work still needs to be done to quantify this dependence.

MacFarlane & Cassinelli (1989) have considered a phenomenological model in which they artificially perturb the driving force in order to investigate the structure and evolution of shocks in the main sequence B star τ Sco. The perturbation gives rise to both a strong forward and reverse shock; this dual shock structure arises because of the method they use to force shock formation. While the MacFarlane and Cassinelli model can be considered as a complementary calculation to the OCR models (since they treat the two shocks correctly but not the full hydrodynamical problem — the opposite of OCR) it is worth noting that the presence of a strong forward shock is inconsistent with the OCR shock picture. Because of the low densities the model is not directly applicable to ζ Pup.

3. Observations and data reduction

A detailed description of the ROSAT satellite and its instrumentation is given in the ROSAT users guide (1991), by Trümper (1983), and by Pfeffermann et al. (1988). We used the PSPC (Position Sensitive Proportional Counter) which has a spectral response from 0.1 to 2.5 keV and a resolution, R, of

$$R = \frac{E}{\Delta E} = 2.33 \left(\frac{E}{0.93}\right)^{0.5} \quad (1)$$

The spatial resolution is approximately 25″ at 0.93 keV .

Two independent PSPC observations of ζ Pup were obtained, with observation details summarized in Table 1. The second of these was obtained specifically for variability studies, and will be the subject of another paper (Baade et al. 1993).

All reduction was performed using the EXSAS reduction package running under MIDAS on a VMS system. The reduction procedure is essentially that outlined in the EXSAS users guide. The extracted spectrum for ζ Pup was corrected for vignetting, coincident correction, and background. The source counts were extracted from a cell of radius 1.7′, while the background cell extended to approximately 14′. In the 60 ksec observations, several weak sources in the background region were excluded.

Several tests were performed examining the sensitivity of the spectra and spectral fitting to the reduction procedure. Extraction of the ζ Pup spectrum from radius 3.3′ primarily affected only the lowest (< 18) pulse height channels, where the background signal is highest. Even then the variation was sufficiently small, and confined, that the spectral fits were not modified.

A basic philosophy of EXSAS is that the observed spectrum should not be corrected for the instrumental response — rather the theoretical spectrum (corrected for interstellar extinction) should be convolved with the instrumental response and compared with that observed. This is the philosophy adopted throughout this paper.

Table 1. Observation summary

observation date	t(secs)	boron Filter	cnts/s	bgnd cnts/s/arcsec^2
24-Apr-1991	1843	Y	0.59	6.2×10^{-8}
19/30-Apr-1992	56651	N	1.26	5.2×10^{-7}

4. The model

Since no definitive model for the production of X-rays in O star stellar winds exists, we decided to adopt the following heuristic approach. In analogy with the OCR model, which in our opinion (see Sect. 2) appears to be the most promising model to explain the origin of X-rays from O stars, we assume that the X-rays arise from a 'uniform' distribution of sources in the stellar wind above some minimum radius R_{min}. These sources are characterized by a temperature T_s, and filling factor e_s. We shall further assume (primarily for discussion purposes) that the density of material entering the shock is given by the ambient wind density, while the density of the post-shock material, as determined from the jump conditions for a strong adiabatic shock, is 4 times this value.

The filling factor e_s is defined such that the emission (ϵ_ν) from a volume element dV is given by

$$\epsilon_\nu = 16 e_s^2 N_p N_e \Lambda_\nu \, dV \quad \text{erg s}^{-1} \quad (2)$$

where Λ_ν is the frequency dependent volume emission coefficient (per electron and proton) of an X-ray plasma calculated using the Raymond-Smith code (Raymond & Smith 1977; Raymond 1988), N_p is the ionized hydrogen density of the ambient wind, and N_e the electron density.

Alternative definitions of the filling factor are possible (we use $16e_s^2$ in our modeling) but we believe the above to be most physical, since with this definition e_s can be regarded as the fraction of the wind that has been shocked to a temperature T_s. For simplicity (both computational and interpretative), we assume a constant filling factor and temperature (within a shock and for all shocks), and compute Λ_ν at a single electron density of 10^{10} cm^{-3} — the dependence of Λ_ν on density, however, is small.

A minimum cut-off radius for the X-ray emission is expected on the basis of the OCR models. Close to the star the radiation line driving instability is effectively dampened by the diffuse radiation field, and hence there are no shocks to produce the X-ray emission. Since the hydrodynamical models still make many untested assumptions no reliable estimate for the cut-off radius is available. Current models by Cooper & Owocki (1992) and Feldmeier (see Puls et al. 1992) indicate R_{min} values of 1.1 to $1.3R_*$. This is additionally supported by diagnostic arguments concerning the structure of the O VI resonance lines (Pauldrach et al. 1993).

To compute the observed spectrum it is necessary to allow for absorption by the "cool" unshocked stellar wind, which requires an atmospheric model. Two atmospheric models for ζ Pup were considered. These are based on the stationary radiation driven wind theory of stellar winds, however, they also take into account the influence of radiation arising from shocked matter (Pauldrach et al. 1993). The parameters (summarized in Table 2) are identical for the 2 models, however the ionization structure has been calculated differently. In model 1 (M1), an attempt was made to take into account the strong line blocking that occurs in the region around the He II resonance lines. The blocking causes He^{++} to recombine in the outer regions of the stellar wind (beyond $0.825V_\infty[5.5R_*]$). In the second model (M2), the line blocking effect is approximated by the corresponding Kurucz model (Kurucz 1979) which has considerably weaker blocking, and hence He remains doubly ionized. Pauldrach et al. (1993) show that the first model provides a better fit to the Si IV, C III, N III, O, and He II(164.0nm) UV lines in ζ Pup.

As shown in Fig. 1, the two models are characterized by very different X-ray absorption properties indicating that the fraction of X-rays (defined to have E> 0.1keV) that escape to

Table 2. Parameters for ζ Pup model

Parameter	Value
d	440 pc
$\dot{M}$	$5.0 \times 10^{-6}\, M_{\odot}\, \mathrm{yr}^{-1}$
R_*	$19.0\, R_{\odot}$
V_{∞}	$2200\, \mathrm{km\, s}^{-1}$
T_{eff}	42500 K
N(He)/N(H)	0.12
N(C)/N(H)	0.00017
N(N)/N(H)	0.00083
N(O)/N(H)	0.00066
$\log N_H(\mathrm{cm}^{-2})_{\mathrm{i.s.}}$	20.0 ± 0.05

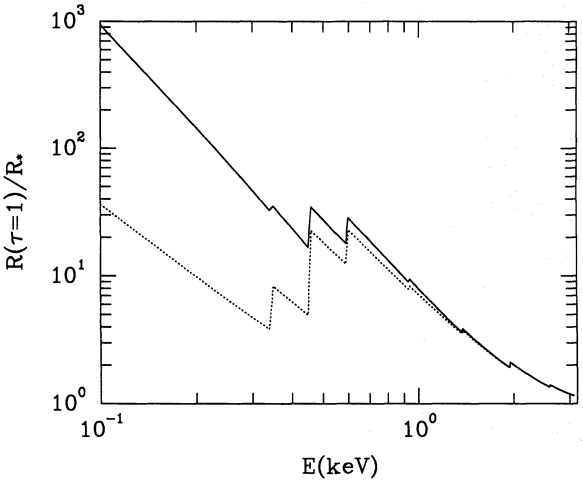

Fig. 1. Radius of optical depth unity as a function of X-ray energy. (solid - Model 1; dashed - Model 2). The observed X-ray flux scales approximately as the inverse of R(τ = 1). Note the strong K shell edge (near 0.5 keV) due to nitrogen, whose abundance is considerably enhanced over solar values (see Table 2)

the observer will be sensitive to the model. In M2, the softer X-rays can originate much deeper than in M1, while at higher energies (> 1 keV) there is little difference between the 2 models. Notice also that the contrast between the K shell edges and the mean opacity is much less in M1 — the K shell absorption, if present, should be much more apparent in the M2 models.

The cool wind opacity is computed fully in NLTE by including the contribution of 26 atomic species in 144 ionization stages (see Pauldrach 1987; Pauldrach et al. 1993). To simplify the radiative transfer, and to allow a rapid exploration of parameter space, we made a simple numerical fit of these opacities to yield

$$\chi_{\nu}^{\mathrm{cool}} = 18.5\rho \left(\frac{\lambda}{2.5\mathrm{nm}}\right)^{2} \quad \mathrm{cm}^{-1} \tag{3}$$

in the layers where helium is doubly ionized ($V(r) < 0.825 V_{\infty}$), and

$$\chi_{\nu}^{\mathrm{cool}} = 18.5\rho \left(\frac{\lambda}{2.5\mathrm{nm}}\right)^{2.8} (1 + 39.66[V/V_{\infty} - 0.825]) \quad \mathrm{cm}^{-1} \tag{4}$$

for the region where He^{++} has recombined to He^{+}. In Eqs. (3) and (4) ρ is the mass density in $\mathrm{g\, cm}^{-3}$, λ the wavelength, and V(r) and V_{∞} are the local and terminal velocities respectively. In the models without recombination we adopted (3) throughout the wind. These fits only apply for ζ Pup.

As a further simplification we adopted an analytical velocity field

$$V(r) = V_{\infty}(1 - 0.989 R_*/r)^{\beta} \quad r > \mathrm{R_{min}} \tag{5}$$

which, via the continuity equation, determines the density. For β = 0.8 to 1.0, the analytical velocity law closely approximates the numerical calculations by Pauldrach et al. (1993). We adopted β = 1.0.

In addition to the cool wind opacity described by (3) and (4) (which is for the valence electrons only) we need to include the K shell opacity of the metals. We have done this for C, N,O, Ne, Mg, Si and S using the cross-sections published by Daltabuit & Cox (1972), and the abundances obtained by Pauldrach et al. (1993) from their fit of the UV spectrum (see Table 2). For simplicity it was assumed that all K shell absorbing ions are in one dominant ionization stage (IV for C to Mg and V for Si and S). This is a good approximation for the X-ray opacities since the energy shifts of the cross-sections are small compared with the spectral resolution of ROSAT.

With the above approximations and assumptions we computed the expected X-ray spectrum by solving the radiative transfer equation in spherical geometry. The comparison of the theoretical spectrum with that observed also requires information about the interstellar absorption. From the fit of the interstellar Ly-α line in the UV spectrum of ζ Pup an interstellar column density of $\log N_H = 20.0 \pm 0.05$ was obtained by Shull & Van Steenberg (1985), and by Kudritzki et al. (1991). This value was adopted for all model comparisons. A change in $\log N_H$ of ± 0.1 (i.e., 2σ) influences only the lowest energy bins (E< 0.3 keV), and does not significantly affect the analysis. For the interstellar X-ray absorption cross sections we adopted the standard values taken from Morrison & McCammon (1983).

4.1. Model with recombination

4.1.1. One component fit

For a single component fit, the 2 free parameters to be determined from fitting the model to the observations are the filling factor e_s and the shock temperature (T_s). The best fit has been determined from the minimum of the χ^2 value using the photon counting errors. For observations with the boron filter, photon statistics are probably the most significant source of error, and hence the deduced χ^2 values have statistical significance. For the observations without the boron filter, the deduced χ^2 values should be regarded as a fitting parameter only, since other sources of error are also important. With the binning adopted, the highest signal-to-noise ratio is 1.5%, however calibration errors will be much larger than this. While calibration errors can

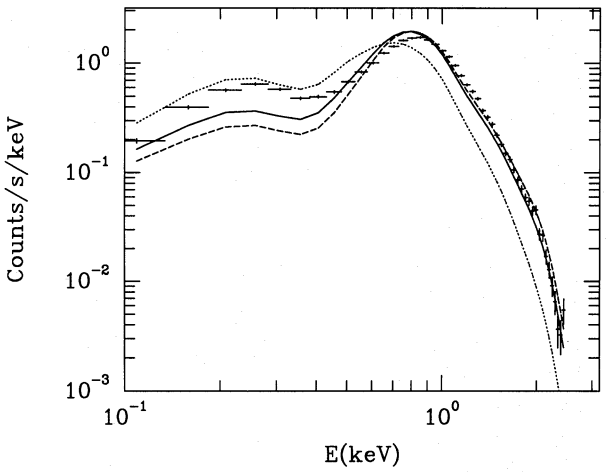

Fig. 2. Comparison of observations (horizontal intervals with error bars) with the predicted X-ray flux from M1 assuming R_{min} = 1.5. Model fits with log T_s = 6.4 (dotted line) or log T_s = 6.6 (dashed line) approximately bracket the observations. The best fit model (solid line), with both the shock temperature and filling factor treated as free parameters, has log T_s = 6.54. The fits suggest that the X-ray emission from ζ Pup can be characterized by temperatures of 3 to 4 × 10^6 K corresponding to shock velocities of approximately 500 km s^{-1}

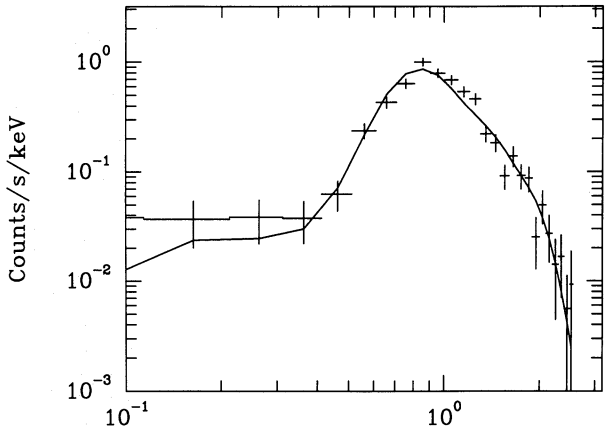

Fig. 3. Similar to Fig. 2, but for observations with the boron filter. The best fit has log T_s = 6.67 with a reduced χ^2 of 2.1. The quality and nature of the fits are consistent with those given for the observations without the boron filter

be estimated, their inclusion is not trivial because they are not statistically independent from bin to bin. Tests, in which we artificially boosted the noise, indicate that the deduced parameters are insensitive to the fitting procedure.

In Fig. 2 we show the fit to the observed data (no boron filter) for model M1 using a radius of $R_{min} = 1.5R_*$, corresponding to a wind velocity of $0.5V_\infty$, and a shock temperature of log T_s = 6.54. The fit is reasonable at high energies, but significantly underestimates the flux at energies below 0.4 keV . The reduced value of $\chi^2$is 60, which is in part due to the very high signal-to-noise of the observations.

An insight into the quality of the model can be gleaned by examining fits (with the filling factor as the only free parameter) on either side of the best determined shock temperature. For log T_s = 6.4, the model fit matches the X-ray flux at very soft energies (Fig. 2), but is very discrepant at high energies. On the other hand, a model with log T_s = 6.6 can match the observations at high energies, but is very discrepant in the soft energy band. This suggests that a 2 component plasma might provide a better fit to the data. The requirement for an extra component is to be expected — we would not expect the shocks to be characterized by a single temperature.

The fits to the observations with the boron filter (Fig. 3) are consistent with the "no boron" fits, although the boron data favors a slightly higher shock temperature of log T_s = 6.67. Better quality boron data, in conjunction with observations without the filter, might provide tighter constraints on the X-ray spectrum at low energies.

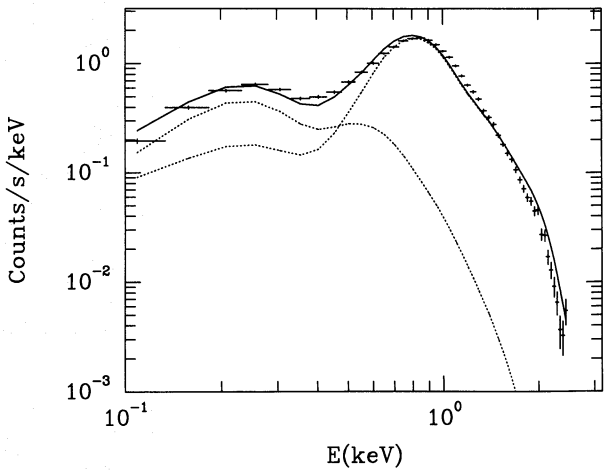

Fig. 4. Comparison of observations (horizontal intervals with error bars) with the predicted X-ray flux from M1 assuming R_{min} = 1.5, and thermal emission that can be characterized by 2 distinct filling factors and temperatures. The best fit has log T_s = 6.66 and e_s = 0.021 for the hotter component, and log T_s = 6.23 and e_s = 0.018 for the cooler component. The individual contributions of the two components are shown by the dotted line

4.1.2. Two component fit

As a single component model does not provide a good fit at all energies we decided (with much hesitation because of the increase in the number of free parameters) to make a 2 component fit. For a given value of R_{min}, we assume that the X-ray emission originates from two plasmas, each specified by its own filling factor and shock temperature. The best fit is shown in Fig. 4, and has a reduced χ^2 of 11. As can be seen from the figure the fit is excellent.

The hotter component has log T_s = 6.66 and e_s = 0.021 and accounts for 55% of the emitted flux. However, because of the attenuation of the wind, the hotter component accounts for

approximately 75% of the X-ray flux incident on the Earth. The cooler component has $\log T_s = 6.23$ and $e_s = 0.018$.

No unique interpretation can be given to the parameters deduced from the 2 component fits. As mentioned previously, we would not expect the shocks to be characterized by a single temperature. Consequently the requirement of a 2 component plasma could merely reflect the fact that the spectrum of a single temperature thermal plasma does not match that of a realistic shock in which a range of temperatures are present. Alternatively, the two components could indicate, as is likely, that there is a distribution of shock strengths — a distribution which may vary with radius.

Because the temperature of the hotter component is very similar to that deduced for the single component model (6.66 compared to 6.54), we can be fairly confident that X-rays for ζ Pup, with energies greater than approximately 0.8keV , come from shocks characterized by $\log T_s$ in the range 6.5 to 6.8.

We have also performed 2 component fits to the boron data. Because of the limited spectral response at very soft energies, we fixed the parameters of the cooler component to be those found in the fit to the observations without the boron filter. The deduced shock parameters of the hotter component are consistent with the values found above.

4.1.3. Sensitivity of fits to R_{min}

We have examined the sensitivity of the fits to the adopted value of R_{min}. Fits with $R_{min} = 2R_*$ are essentially indistinguishable from those with $R_{min} = 1.5R_*$ (both single and 2 component).

Single component fits with $R_{min} = 10R_*$ (Fig. 5) are, however, significantly poorer than with the smaller R_{min} values — the minimum χ^2 values are a factor of 2 higher. This behavior is easily understood from the variation of $R(\tau = 1)$ with wavelength.

The observed X-ray flux at a given energy can be assumed to arise at those radii where $\tau < 1$. When the adopted minimum radius is smaller than $R(\tau = 1)$, the X-ray fluxes will be insensitive to its exact value. Only when the minimum radius is comparable to, or larger than, $R(\tau = 1)$ will the X-ray fluxes depend on its value. In the recombination models $R(\tau = 1)$ is greater than $2R_*$ for E < 2 keV (see Fig. 1), hence the X-ray fluxes are not very sensitive to the choice of R_{min} when it is less than $2R_*$. On the other hand, for R_{min}=$10R_*$, the predicted X-ray fluxes for E> 1 keV are significantly reduced relative to the $R_{min} = 1.5R_*$ model.

With a two component fit the additional two free parameters allow us to get a fit which is as good, if not better, than that for $R_{min} = 1.5R_*$. The best fit has $\log T_s = 7.07$ and $e_s = 0.019$ for the hotter component, and $\log T_s = 6.39$ and $e_s = 0.026$. Because of the absence of X-ray emission from inside $10R_*$, the deduced temperatures are considerably higher than those obtained for R_{min}=$1.5R_*$.

It is difficult to understand why the X-ray emission should be limited to radii beyond $10R_*$. Thus while we can obtain a fit, we believe the derived temperatures have little physical significance, and prefer those deduced from the two component fit with R_{min}=$1.5R_*$.

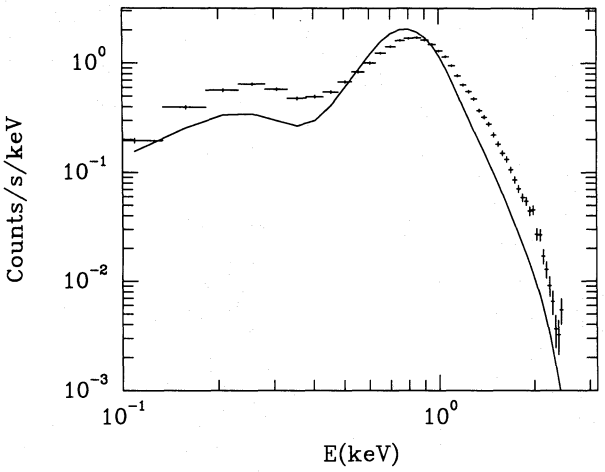

Fig. 5. Comparison of observations (horizontal intervals with error bars) with the predicted X-ray flux from M1 assuming $R_{min} = 10.0$. The best fit model with $\log T_s = 6.57$ is shown, and is very discrepant, particularly for E> 1 keV . The X-ray fluxes for $E < 1$ keV are not significantly affected by the larger R_{min} value — an even larger R_{min} value would be required to reduce the flux at these energies

4.1.4. Comparison with earlier work

Our values describing the X-ray spectrum of ζ Pup can be compared with those found by Cassinelli et al. (1981), who used the code of Raymond-Smith (1977) to fit (optically-thin) thermal spectra to the spectrum of several O and B supergiants. For ζ Pup, best consistency with the data was found for an embedded source model with $\log T_s = 7.1$ and $\log N_H = 21.4$. The higher N_H value indicates that significant intrinsic absorption (i.e., not interstellar) must be present. Their fit was poorly constrained, and their deduced shock temperature is much higher than our best fit value for the M1 model (but we note that their 90% confidence limit does extend to $\log T_s = 6.6$). We believe this emphasizes the need to use a reliable wind model in order to constrain the properties of the X-ray emitting gas. In addition, the enhanced X-ray resolution and soft energy sensitivity of ROSAT over *Einstein* allows (for a given model) much tighter constraints on the characteristics of the X-ray emission.

The observed X-ray luminosity agrees closely with the *Einstein* value of 1.1×10^{-11} erg cm^{-2} s^{-1} (no interstellar absorption correction) published by CHS. The correction to the observed X-ray flux, for the effects of interstellar absorption, is less than 5%. Note that because of the low resolution of the *Einstein* and ROSAT observations, the correction of the observed count-rate to an X-ray flux is model dependent.

In Table 3 we summarize the parameters of the different model fits. The quantity $F_X(obs)$ is the observed X-ray flux as computed from the model fluxes, while F_X(thin) is the X-ray luminosity we would observe if the wind was optically thin. When the temperature is in "[ ]", it was held fixed during the

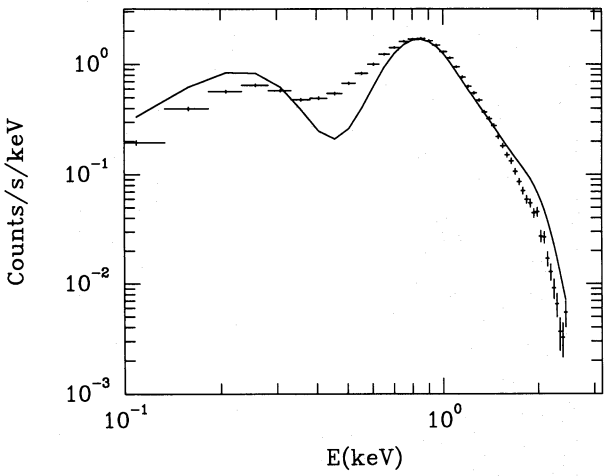

Fig. 6. Comparison of observations with the predicted X-ray flux from M2 assuming R_{min} = 1.5. The best fit model with $\log T_s$ = 6.83 is illustrated. The most striking discrepancy between the model and observed fluxes is the presence of the strong absorption, due to the K shell of nitrogen, at 0.5 keV in the model fluxes. This discrepancy occurs in all fits, independent of R_{min}

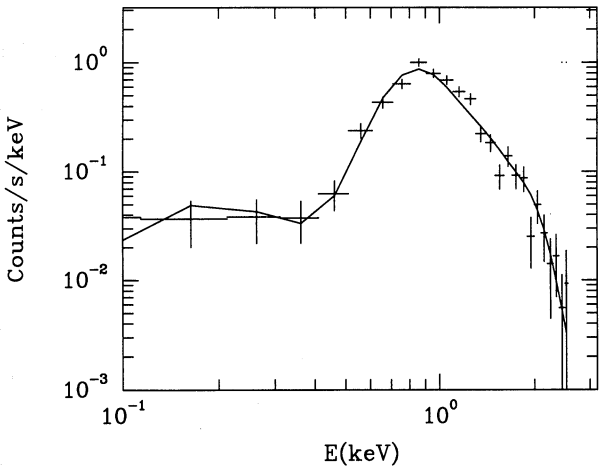

Fig. 7. Comparison of the observations (with boron filter) with the predicted X-ray flux from M2 assuming R_{min} = 1.5. The best fit model with $\log T_s$ = 6.79 is illustrated. No discrepancy is apparent in the fit, which primarily reflects the lack of transmission of the boron filter around the nitrogen K shell edge

fitting procedure. In some cases we provide models on either side of the best fit model in order to illustrate the sensitivity of the fit.

4.2. Model without recombination

We saw in the previous section that the recombination model with $\log T_s$ in the range 6.5 to 6.7 could provide a reasonable fit to the observed X-ray fluxes of ζ Pup. It is now pertinent to examine how well the X-ray fluxes can be fitted for the atmospheric model, M2, in which helium is always doubly ionized.

Qualitatively the fits are much poorer than those obtained with model M1. The best fit is obtained for $\log T_s$ = 6.83 (Fig. 6), and has a χ^2 value roughly a factor of 2 larger than the best model fit for M1. However, it is the nature of the discrepancy which suggests that the M1 models are more viable than the M2 models. In particular we see the models possess a strong absorption at 0.5 keV due to K shell absorption by nitrogen, which is definitely not present in the data.

The discrepancy of the M2 predictions with observation is further emphasized if we allow for the possibility that we have 2 different temperatures plasmas present. Unlike the M1 models, *there is no improvement in the fit*. This is understandable since the biggest discrepancy arises from the presence of K shell absorption in the models — absorption which will be present in all models independent of the shock temperature.

For completeness, we also illustrate the best fit of M2 to the observations with the boron filter (Fig. 7). No discrepancy of the model with observation is apparent, reflecting the insensitivity of the boron observations to the X-ray flux around the nitrogen K shell absorption edge. This agreement further emphasizes the importance of low N_H objects like ζ Pup for understanding X-ray production in O stars.

5. Shock structure, cooling lengths, etc

Before attempting to understand the implications of our findings, it is worthwhile to give some useful formulae regarding the density of ζ Pup's wind, and the structure of the shocks. These are presented in a slightly different form from other discussions in the literature, allowing us to emphasize some important points not previously alluded to.

The shock temperature can be expressed as

$$T_s = 2.3 \times 10^5 \frac{\mu}{(1+\gamma)} \left(\frac{U_O(\mathrm{km\,s^{-1}})}{100} \right)^2 \qquad (6)$$

(e.g., Dyson & Williams 1980) where U_O is the velocity (relative to the shock) of the material flowing into the shock, μ is the mean ionic weight and γ is the ratio, by number, of electrons to ions. The above formula assumes that the pre-shock gas is fully ionized. The ambient ion density in the wind is given by

$$N_i = \frac{6.234 \times 10^{12}}{\mu} \left(\frac{R_\odot}{r} \right)^2 \left(\frac{\dot{M}(M_\odot\,\mathrm{yr^{-1}})}{10^{-6}} \right) \left(\frac{1000}{V(\mathrm{km\,s^{-1}})} \right), \qquad (7)$$

The immediate post shock density, for a strong shock, is a factor of 4 higher.

To estimate the cooling time t_c we use

$$t_c = \frac{1.5(1+\gamma)\,k\,T_s N_i}{4 X_p N_e N_i \Lambda_{RS}(T)} \quad . \qquad (8)$$

where X_p is the ionic fraction of ionized hydrogen and Λ_{RS} is the cooling function. In the range $T = 10^6$ K to 10^7 K we can approximate Λ_{RS} by

$$\log \Lambda_{RS}(\odot) = -18.55 - 0.55 \log T \qquad (9)$$

Table 3. Model summary

Model	boron	R_{min} (R_*)	log $T_s(K)$	ϵ_s	F_X(obs) (10^{-11} erg cm^{-2} s^{-1})	F_X(obs)/F_X(thin)	χ^2/n
M1	N	1.5	[6.4]	0.031			242
M1	N	1.5	6.54	0.027	1.35	0.019	60
M1	N	1.5	[6.6]	0.024			75
M1	Y	1.5	6.67	0.020	1.06	0.026	2.1
M1	N	2.0	6.54	0.027	1.30	0.036	66
M1	N	1.5	6.23 / 6.66	0.018 / 0.021	1.44	0.018	19
M1	N	1.5	6.32 / [6.80]	0.022 / 0.015	1.56	0.018	24
M1	N	2.0	6.30 / 6.81	0.021 / 0.016	1.52	0.036	15
M1	N	10.0	6.39 / 7.07	0.026 / 0.019	1.53	0.27	7
M2	N	1.5	6.83	0.015	1.26	0.046	105
M2	Y	1.5	6.79	0.015	1.23	0.044	1.9

which is taken from the cooling curve given by Rosner et al. (1978). We use this formulation, rather than the more precise one given by Rosner et al. as it is a single parameterization in the range of interest — the small additional errors in the fit are irrelevant for our purposes.

In many cases we will be interested in sources that have evolved surface abundances. If the cooling is dominated by the non CNO metals (e.g., Fe) then we can assume that the cooling per gram is approximately independent of both the H/He ratio and the CNO abundances. In this case we can write

$$\Lambda_{RS} = \left(\frac{\mu}{\mu_\odot}\right)\left(\frac{Xp_\odot}{Xp}\right)\Lambda_{RS\odot} \quad (10)$$

The same expression also holds if free-free cooling from H and He^{++} is dominant. In terms of the shock velocity U_O, the cooling function is

$$\Lambda_{RS} = 2.24\times10^{-22}\left(\frac{\mu}{Xp}\right)\left(\frac{1+\gamma}{\mu}\right)^{0.55}\left(\frac{100}{U_O(\mathrm{km\,s^{-1}})}\right)^{1.1} \quad (11)$$

On combining Eqs. (6), (7), (8) and (11) the cooling time is given by

$$t_c = 0.00835\left(\frac{\mu}{\gamma}\right)\left(\frac{\mu}{1+\gamma}\right)^{0.55}\left(\frac{r}{R_\odot}\right)^2\left(\frac{10^{-6}}{\dot{M}(M_\odot\,\mathrm{yr^{-1}})}\right)\left(\frac{V(\mathrm{km\,s^{-1}})}{1000}\right)\left(\frac{U_O(\mathrm{km\,s^{-1}})}{100}\right)^{3.1}\ \mathrm{s} \quad (12)$$

The cooling length (l_c) (which is the length of hot post-shock material behind the shock) is given by

$$l_c = U_O t_c/4 \quad (13)$$

where $U_O/4$ is the velocity of the post-shock material relative to the shock. Combining this expression with that for t_c (Eq. 12) gives

$$l_c = 3.0\times10^{-7}\left(\frac{\mu}{\gamma}\right)\left(\frac{\mu}{1+\gamma}\right)^{0.55}\left(\frac{r}{R_\odot}\right)^2\left(\frac{10^{-6}}{\dot{M}(M_\odot\,\mathrm{yr^{-1}})}\right)\left(\frac{V(\mathrm{km\,s^{-1}})}{1000}\right)\left(\frac{U_O(\mathrm{km\,s^{-1}})}{100}\right)^{4.1} R_\odot. \quad (14)$$

Krolik & Raymond (1985) note that there are 2 basic shock structures which they term 'optically thin' and 'optically thick', but these are termed 'non-radiative' and 'radiative' shocks in the notation of McKee & Hollenbach (1980). In the non radiative shock the cooling time is long, the shocked material never cools, and the plasma can be characterized by a single temperature. On the other hand in a radiative shock the cooling time is very short, and a range of temperatures and ionization states will exist. Krolik & Raymond (1985) define the shocks in terms of a minimum column density for cooling. Their minimum column density is approximately given by $4l_cN_i$(wind).

The cooling length, in conjunction with the ionization structure output by the Raymond-Smith code, can be used to provide a crude estimate of the optical depth in some of the more important cooling line. Although self absorption may occur for some lines the optical depths are generally not sufficiently large to drastically alter the cooling - most of the absorbed photons are merely scattered, not destroyed.

In practice our simple estimate of the cooling length breaks down when the cooling time becomes comparable to the flow time (=r/v). Adiabatic cooling must also be considered — its time scale is given approximately by the flow time.

The relative cooling lengths and time scales for ζ Pup, with $U_O = 500\,\mathrm{km\,s^{-1}}$ and $T_s = 3.6\times10^6$ K, are summarized in Table 4.

Inside $2R_*$, the cooling time is over a factor of 60 smaller than the flow time, suggesting that the dynamical model and isothermal shocks considered by OCR may have some validity.

Table 4. ζ Pup time scales

r/R_*	V(r) km s^{-1}	N_i(wind) cm^{-3}	t_c s	t_{flow} s	l_c/r
1.5	750	3.8×10^{10}	14	2.7×10^4	9.0×10^{-4}
2.0	1110	1.4×10^{10}	375	2.4×10^4	0.0018
5.0	1765	1.4×10^9	3.7×10^3	3.7×10^4	0.0070
10.0	1980	3.3×10^8	1.7×10^4	6.7×10^4	0.016
50.0	2160	1.2×10^7	4.5×10^5	3.1×10^5	0.086
100.0	2180	2.9×10^6	1.8×10^6	6.1×10^5	0.17

The cooling time, however, increases rapidly with radius. Beyond $10R_*$, the cooling time is comparable to the flow time and the simple OCR model will break down.

The cooling times and length scales in Table 4 assume that the shocks interact with material whose properties can be characterized by the steady state flow. On the other hand, the OCR calculations show that the line instability completely disrupts the flow so that most of the mass loss occurs in dense shells, with low density (compared to the steady state flow) high velocity gas between them. Consequently, the high velocity material entering the (reverse) shock is of lower density than the mean flow, and hence the cooling times will be correspondingly even larger than those given in Table 4.

Several other points are worth noting. First, there is a very strong dependence of the cooling time on the shock velocity. Making the reasonable assumption that the shock velocity scales as the terminal velocity we note that the cooling length will scale as the 5th power of the terminal velocity.

Second, in stars with low mass loss, such as τ Sco the assumption of radiative shocks will become invalid much closer to the star – for τ Sco (R=6.7$R_\odot$, $\dot{M} \approx 10^{-8} M_\odot$ yr^{-1}, Lamers & Rogerson 1978) the l_c/r ratio, for a given r/R_*, is increased by a factor of 180! Such objects might be expected to show different X-ray properties.

Finally, due to the higher mass loss rates and smaller radii, shock cooling in WR stars is much more efficient. From (14) and using (11) we note that

$$\frac{l_c}{r} \propto \left(\frac{\mu}{\gamma}\right)\left(\frac{\mu}{1+\gamma}\right)^{0.55}\left(\frac{R_*}{R_\odot}\right)\left(\frac{V(\mathrm{km\,s^{-1}})}{1000}\right)\left(\frac{10^{-6}}{\dot{M}(M_\odot\,\mathrm{yr}^{-1})}\right)\left(\frac{r}{R_*}\right) \quad (15)$$

and for a typical WNE star (with μ = 4, R_*=3$R_\odot$, $\dot{M}$ = $5 \times 10^{-5}\, M_\odot$ yr^{-1}, and V = 2000 km s^{-1}) the ratio of l_c to the local radius is a factor 25 smaller at a given value of (r/R_*). As a consequence, the isothermal shock approximation made by OCR is more valid for WR stars than O stars. The velocity/density structure predicted by the OCR models may therefore be more relevant to WR stars, even though continuum transfer is neglected. It is interesting to ask whether the momentum problem in WR stars, and the absence of a similar problem for O stars, are related to the different shock structures.

6. Discussion

With a simple parameterization of the true X-ray opacity, and assuming that the X-rays arise from shocks uniformly distributed throughout the wind, we have modeled the X-ray spectrum of the O4f star ζ Pup. The best fit, single component model, occurs when He^{++} recombines to He^{+} in the outer regions of the stellar wind, as predicted by recent detailed cool wind model calculations. A shock temperature of T_s(K) = 6.54, and a filling factor of around 3% are deduced. Due to absorption by the stellar wind (and to a minor extent by stellar occultation) less than 5% of the total emitted X-ray flux escapes the star.

An improved fit is obtained when we consider two components, each characterized by its own filling factor and temperature. The deduced temperatures of the 2 components are log T_s = 6.23 and log T_s = 6.66. The similarity between the deduced temperature for the hotter component, and that found in the single component fit, indicates that the X-ray emission at energies greater than 1 keV can be characterized by shock velocities of approximately 500 km s^{-1}.

In models without recombination, the fits were significantly poorer. A significant K shell absorption is seen in these models, but is definitely not present in the observational data. *No improvement* in the fit is seen when we allow for two components.

The analyses suggest that the X-ray flux provides an invaluable diagnostic of the ionization of helium in the stellar wind in stars of low reddening. The computation of the helium ionization structure is extremely difficult as it is very dependent on the wind structure, the UV blanketing around the He II Ly-α resonance line, and the X-ray flux itself.

One important issue to address is the requirement that the soft X-rays originate at very large radii ($> 100R_*$ in the recombination model, see Fig. 1). In the literature it has been generally assumed that the shocks do not form beyond several stellar radii, although the OCR models do not consider this scenario. Calculations that address the shock behavior at large radii are urgently needed. At radii where the soft X-ray flux originates, adiabatic cooling is important, and constrains any model in which the hot gas originates at smaller radii.

The requirement that significant X-ray flux be emitted at large radii is not new — it is needed to explain the X-ray emission from WR stars whose stellar winds are very opaque to X-rays (Pollock 1987).

One obvious question to ask is whether the shock velocities we determine can be directly related to some observed property of the star — the most obvious parameter being the turbulent velocity measured in the fitting of UV P Cygni profiles.

Present time dependent calculations of hot star winds suggest that the maximum velocity reached in the wind is typically of the order V_∞+U_O, where V_∞ is the terminal velocity of the corresponding stationary model (Owocki 1992). Hence the difference between the edge velocity (V_e) and V_∞ should yield, approximately, the shock velocity.

On the other hand, UV profile fits allowing for an artificial turbulence (e.g., Groenewegen & Lamers 1989) show for a saturated profile that

$$\frac{(V_e - V_\infty)}{V_t} \approx 2 \qquad (16)$$

where V_t is the turbulence derived in the outer regions of the line formation region. Thus, $U_O \sim 2V_t$, a relationship supported by our investigation since the measured turbulence for ζ Pup is 250km s^{-1} (Stefan Haser, private communication). The above relationship between deduced X-ray shock temperatures and turbulent velocities can be easily tested by future X-ray modeling of stars showing a range in turbulent velocities.

The high quality ROSAT data provide additional information that can be used in modeling the wind of ζ Pup. Pauldrach et al. (1993) included the influence of X-rays, and the associated radiation field, in their analysis of ζ Pup, however they fixed the shock temperature via the turbulent velocity indicated by UV resonance lines, and adjusted the filling factor so that the emitted X-ray flux matched that observed by *Einstein*. As a consequence their final model is not fully consistent with the X-ray data presented here. The next step is clearly to repeat the spectral analysis of Pauldrach et al. (1993), but this time constraining both the shock temperature and emission measure so that the emergent X-ray spectrum is consistent with the observed ROSAT spectrum of ζ Pup.

From the M1 model fitting we deduced that the emergent X-ray flux, particularly at soft energies (i.e., < 1 keV), was insensitive to the choice of R_{min}. Unfortunately , the soft X-ray flux can have an important influence on the local ionization structure, and hence is important for modeling of UV wind lines. Since constraints on the soft X-ray flux arising deep in the atmosphere cannot be deduced from the X-ray observations, they can only be deduced from their effect on UV and optical spectra. In order to reduce the number of free parameters, theoretical guidance on the behavior of the shock structure and spectrum with radius is urgently needed.

In order to place tighter constraints on the X-ray model parameters, improved X-ray flux calculations are also needed. We have used a single shock temperature, and assumed a constant filling factor. As there will be a distribution in shock strengths, there will be a distribution in shock temperatures. In addition, a radiative shock has a range of temperatures, and hence a spectrum characterized by a single temperature cannot be associated with it. In this regard, future observations, with higher spectral resolution, are critically important. They will provide the ability to look at temperature sensitive lines, and hence remove many of the model ambiguities in our fitting procedure.

Much work needs to be done to understand the X-ray spectrum from O stars. These X-rays provide diagnostics of the dynamics of the stellar wind, and are important in their own right since they influence the ionization structure and hence the observed spectrum. A forthcoming paper (Baade et al. 1993) will address the key issue of variability of the X-ray spectrum of ζ Pup.

ζ Pup is but one of a large number of O stars that have been observed with ROSAT. Detailed analyses of these stars should allow the X-ray emission properties of single O stars to be coupled with the fundamental stellar parameters. As a large fraction of the X-rays is absorbed by the stellar wind, and since the absorption properties themselves depend on the stellar parameters, it is not difficult to see why correlations of X-ray flux with other parameters may have been masked when using observed X-ray fluxes.

Acknowledgements. It is a pleasure to thank the ROSAT team for its support. Without their considerable effort, these observations would not have been feasible. We also gratefully acknowledge the use of the EXSAS reduction package. This work was partially supported by the BMFT(010R9008), and by the DFG "Gerhard Hess program" under grant Pa477/1-1.

References

Abbott, D.C, 1980, ApJ, 242, 1183
Baade, D., Lucy, L.B., 1987, A&A, 178, 213
Baade, D., et al., 1993, (in preparation)
Carlberg, R.G., 1980, ApJ, 241, 1131
Cassinelli, J.P., Olson, G.L., 1979, ApJ, 229, 304
Cassinelli, J.P., Olson, G.L., Stalio, R., 1978, ApJ, 220, 573
Cassinelli, J.P., Swank, J.H., 1983, ApJ, 271, 681
Cassinelli, J.P., Waldron, W.L., Sanders, W.T., Harnden F.R., Jr., Rosner, R., Vaiana, G.S., 1981, ApJ, 250, 677
Chlebowski, T., 1989, ApJ, 342, 1091
Chlebowski, T., Harnden, F.R., Jr., Sciortino, S., 1989, ApJ, 341, 427
Cooper, R.G., Owocki, S.P., 1992, in "Nonisotropic and Variable Outflows from Stars", eds. L. Drissen, C. Leitherer, A. Nota, A.S.P. Conf. Ser, Vol 22, p281
Daltabuit, E, Cox, D.P., 1972, ApJ, 177, 855
Dyson, J.E., Williams, D.A., 1980, "Physics of the Interstellar Medium", Manchester University Press
Groenewegen, M.A.T., Lamers, H.J.G.L.M., 1989, A&AS, 79, 359
Harnden, F.R., Jr, Branduardi, G., Elvis, M., et al., 1979, ApJ, 234, L51-54
Hearn, A.G., 1972, A&A, 19, 417
Krolik, J.H., Raymond, J.C., 1985, ApJ, 298, 660
Kudritzki, R.P., Puls, J., Gabler, R., Schmitt, J.H.M.M., 1991, "Extreme Ultraviolet Astronomy", eds. R.F. Malina, and S. Bowyer, Pergamon Press, p 130
Kurucz, R.L., 1979, ApJS, 40, 1
Lamers, H.J.G.L.M., Rogerson J.B., Jr, 1978, A&A, 66, 417
Long, K.S., White, R.L., 1980, ApJ, 239, L65
Lucy, L.B., White, R.L., 1980, ApJ, 241, 300
Lucy, L.B., 1982, ApJ, 255, 286
Lucy, L.B., Solomon, P.M., 1970, ApJ, 159, 879

Lucy, L.B., 1984, ApJ, 284, 351
MacFarlane, J.J., Cassinelli, J.P., 1989, ApJ, 347, 1090
MacGregor, K.B., Hartmann, L., Raymond, J.C., 1979, ApJ, 231, 514
Mckee, C.F., Hollenbach, D.J., 1980, ARA&A, 18, 219
Morrison, R., McCammon, D., 1983, ApJ, 270, 119
Nordsieck, K.H., Cassinelli, J.P., Anderson, C.M., 1981, A&A, 248, 678
Owocki, S.P., 1992, in ''The Atmospheres of Early Type Stars", eds. U. Heber and C. S. Jeffery, Springer, Berlin, p393
Owocki, S.P., Rybicki, G.B., 1984, ApJ, 284, 337
Owocki, S.P., Rybicki, G.B., 1985, ApJ, 299, 265
Owocki, S.P., Rybicki, G.B., 1986, ApJ, 309, 127
Owocki, S.P., Castor, J.I., Rybicki, G.B., 1988, ApJ, 335, 914 (OCR)
Pallavicini, R., Golub, L., Rosner, R., et al., 1981, ApJ, 248, 279
Pauldrach, A., 1987, A&A, 183, 295
Pauldrach, A.W.A., Puls, J., Butler, K., Kudritzki, R.P., Hunsiger, J., 1993, submitted to A&A
Pfeffermann, E., Briel, U.G., Hippmann, H., etal, 1988, Proc. SPIE, 733, 519
Pollock, A.M.T., 1987, A&A, 171, 135
Puls, J., Pauldrach, A.W.A, Kudritzki, R.P., Owocki, S.P., Najarro, F., 1992, in Rev. in Mod. Astr., Vol. 6 (in press)
Puls, J., Owocki, S.P., Fullerton, A.W., 1993, (in press)
Corona.
Raymond, J.C., 1988, in "Hot Thin Plasmas in Astrophysics", eds. Roberto Pallavicini, Dordrecht, Kluwer Academic Publishers, p3
Raymond, J.C., Smith, B.W., 1977, ApJS, 35, 419
Rogerson J.B., JR, Lamers, H.J.G.L.M., 1975, Nat., 256, 190
Rosner, R., Tucker, W.H., Vaiana, G.S., 1978, ApJ, 220, 643
Rybicki, G.B., Owocki, S.P., Castor, J.I., 1990, ApJ, 349, 274
ROSAT User's Guide, 1991, Max-Planck-Institut für Extraterrestrische Physik, 8046 Garching bei München
Sciortino, S., Vaiana, G.S., Harnden, F.R., JR, et al., 1990, ApJ, 361, 621
Seward, F.D., Forman, W.R., Giacconi R., et al., 1979, ApJ, 234 L55
Shull, J.M., Van Steenberg, M.E., 1985, ApJ, 294, 599
Trümper, J., 1983, Adv. Space Res. 2, 241
Waldron, W.L., 1984, ApJ, 282, 256

This article was processed by the author using Springer-Verlag LaTeX A&A style file version 3.